Evaluating the Impacts of Biological Aspects on CNN Performance in Detecting Harmful Brain Activity

Juliet Kern, Kevin Meng
20832291, 20850348

Abstract

This paper investigates whether or not adding more biological aspects to a Convolutional Neural Network (CNN) causes the network to classify more similarly to humans. For the classification of Electroencephalography (EEG) spectrograms, the biological modifications include lateral connections, feed-forward skip connections, neuron adaptation, and only detecting lines and edges in the first stage. We propose that simulating the human visual system by adding these biological aspects to the CNN will result in better performance by predicting a probability distribution that is more similar to the human experts' vote distribution. A simple CNN model was first created to serve as a baseline for each biologically modified model to be compared to. The experiments included connecting each layer to every subsequent layer to simulate feed-forward skip connections, self-attention layers after convolutional layers to simulate lateral connections, adding L2 regularization to simulate neuron adaptation, and manually setting filters in the first convolutional layer such that they only detect lines and edges to simulate the detections made in the V1 region of the visual cortex. The resulting changes in the network from the integration of feed-forward skip connections yielded significant improvements in both train and validation losses, with only a slight increase in the number of total parameters, demonstrating increased parameter efficiency. The addition of self-attention layers, enabling contextual integration throughout the entire input map and feature enhancement, resulted in the lowest train and validation losses of all the biological modifications. Adding L2 regularization resulted in a decrease in validation loss, but an increase in training loss, and a reduced amount of overfitting. Finally, manually setting a reduced number of filters in the first convolutional layer resulted in slight decreases in training and validation loss. This report is used for educational purposes to better understand how biologically-inspired methods can be used in machine learning to make effective predictions.

1 Introduction

Electroencephalography (EEG) is a method to record an electrogram of the electrical activity of the brain [1]. EEG signals can be used to detect harmful brain activity, leading to diagnoses and eventual treatment of a medical condition [2]. Currently, the analysis of EEG recordings can only be done manually by specialized neurologists. This labor-intensive, error-prone process causes a major bottleneck and is also highly unreliable, as experts often fail to come to a consensus on the correct label of certain EEG segments [3]. As such, the targets in this dataset are vectors containing 6 patterns of interest, one for each brain activity class, determined by the count of expert annotator votes for the corresponding class [3]. An ideal EEG prediction model is able to classify electrical brain activity closely resembling that of the distribution of classifications by

specialized neurologists. This is determined by measuring the divergence from the expected target label distributions, using the Kullback Leibler Divergence function [4][5]. The analysis of EEG spectrograms using a Convolutional Neural Network (CNN) will help promptly detect harmful brain activity, and crucially, since the targets are human-annotated, adding biological features to mimic the human visual system can guide the output probabilities to be increasingly similar to the targets.

1.1 Literature Review

Relations between CNNs and the human vision system have been widely studied. Many aspects of CNNs have been inspired by the visual system, having similar image processing hierarchies [6].

Neuron adaptation has also been introduced to machine learning models in order to mimic biological neurons and enhance model functionality. This adaptation process involves changes in neuron activity over time in response to constant sensory inputs, allowing models to adapt their processing based on the incoming signals. Additionally, it acts as a form of regularization, stabilizing the learning process by adjusting neuron activities closer to a desired state, effectively minimizing the impact of large deviations in neuron activity. By reducing these deviations, adaptation ensures that the network's overall learning trajectory is smoother and more stable, similar to the way biological systems manage to maintain functionality amidst varying visual stimuli [7].

Contextual awareness, or attention in the primate visual system reflects a multiplicative gain based on particular aspects of a visual scene for detailed analysis, while ignoring other aspects [8]. The primate visual system integrates information across the visual field and determines whether to enhance or suppress particular aspects through lateral connections between functional columns of neurons in a cortical area. The enhancement of one feature through lateral connections involves the suppression of nearby or functionally related neurons [9]. Visual attention has also been applied in CNNs to make it flexible and context-dependent for a variety of different applications, such as the application of spatial attention to aid in image captioning [10].

Additionally, current research attempts to bridge the gap between artificial and biological visual systems by incorporating biologically inspired components into CNNs. Recent studies have integrated skip connections into CNNs, identifying the parallels to the neural architectures observed in the brain. The brain's neocortex displays structural similarity to residual networks, where certain neural pathways bypass immediate layers, resembling skip connections in advanced CNN models [11]. Analysis of the moment-by-moment relationship of the neuronal population activity across visual areas showed feed-forward interactions of the V1 leading to the V4, and skipping the V2 [12]. Skip connections are also commonly implemented in various CNN architectures, most notably in ResNet and DenseNet [13].

The LGN-CNN architecture features a first convolutional layer equipped with a single filter designed to emulate the function of the Lateral Geniculate Nucleus (LGN) in the human visual system. This layer uses a filter that exhibits rotational symmetry, effectively capturing the long-range connections and complex behaviors of LGN cells. This biologically inspired approach aims to enhance the CNN's ability to process visual information in a manner more similar to human vision [6].

This report aims to expand upon existing literature that supports modifications to CNN architectures through biological insights. In addition to these developments, this report investigates the integration of biological aspects into the complex medical domain of EEG signal classification.

1.2 Approach

The objective is to create a CNN model to classify EEG spectrograms of harmful brain activity more closely to the classifications done by human experts. The general approach to accomplishing this is by first creating a baseline CNN model, and measuring how closely the probabilities for each brain activity class predicted by the model matches the target probabilities. Upon setting a baseline, individual biological aspects will be added to the baseline CNN model to assess their specific effects. The specific additions to the CNN to mimic aspects of the primate visual system

include lateral connections, feed-forward skip connections, neuron adaptation, and the detection of only lines and edges in the first processing layer/region. All the biological aspects that result in a more similar prediction to the expert annotators will be combined to yield a final model with all beneficial modifications implemented in the CNN.

2 Task and Data

This report evaluates and analyzes the effects that biological aspects have on the performance of a CNN in classifying EEG signals. Included in the dataset are spectrogram data and the count of annotator votes for a given brain activity class [3]. These classes include seizure (SZ), generalized periodic discharges (GPD), lateralized periodic discharges (LPD), lateralized rhythmic delta activity (LRDA), generalized rhythmic delta activity (GRDA), or “other."

Table 1: Brain Activity Class Labels and Example Targets

Brain Activity Class	Example Target
seizure (SZ)	0.00
generalized periodic discharges (GPD)	0.00
lateralized periodic discharges (LPD)	0.25
lateralized rhythmic delta activity (LRDA)	0.00
generalized rhythmic delta activity (GRDA)	0.17
other	0.58

These votes were converted to a target probability tensor that stores the expert annotators’ consensus on EEG signal classifications into brain activity categories. The model’s output predicts the log probability that a given EEG signal corresponds to a specific brain activity class. The classes and an example target are shown in Table 1. Figure 1 demonstrates a sample of the input data used. The dataset containing 11,138 EEG spectrograms was split into a train, validation, and test with a 70-15-15 split.

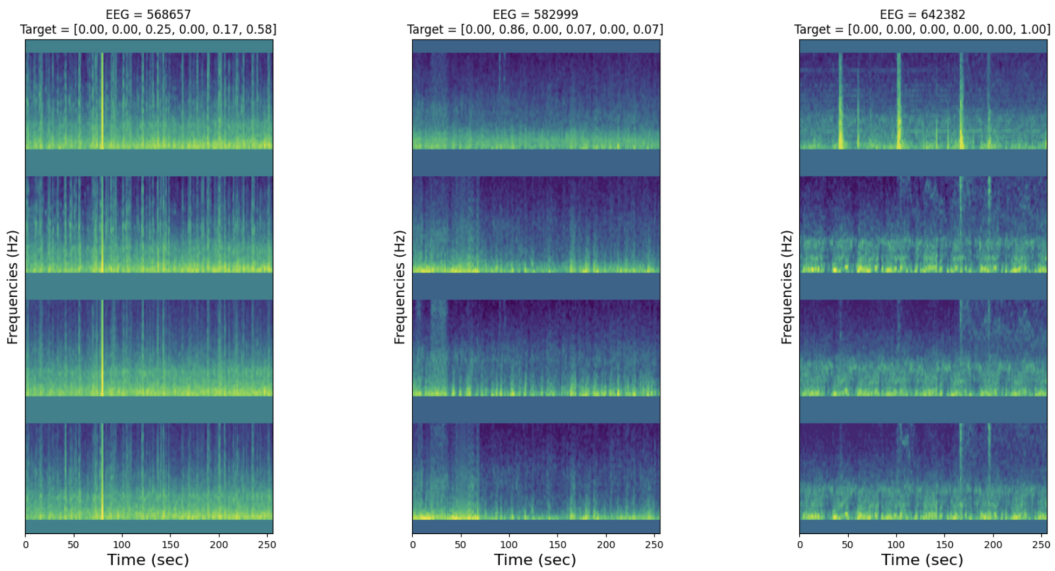

Figure 1: Sample Input and Target values.

3 Methods

3.1 Baseline CNN

A CNN was used for the classification of EEG spectrograms. The CNN was determined to be the optimal model for this task due to its inherent similarities with the primate visual system, most notably with hierarchical processing, and feature extraction with spatial invariance.

Figure 2 demonstrates how visual information is first processed in the V1 region of the brain where simple cells, with excitatory and inhibitory regions arranged to detect simple features such as lines and edges of different orientations, followed by increasingly complex features in the higher visual areas such as shapes detected in V2, and objects detected in V4 [9]. CNNs follow a similar hierarchy when processing images, with each deeper layer composed of filters responsible for detecting increasingly complex features, resulting in hierarchical feature detection as well.

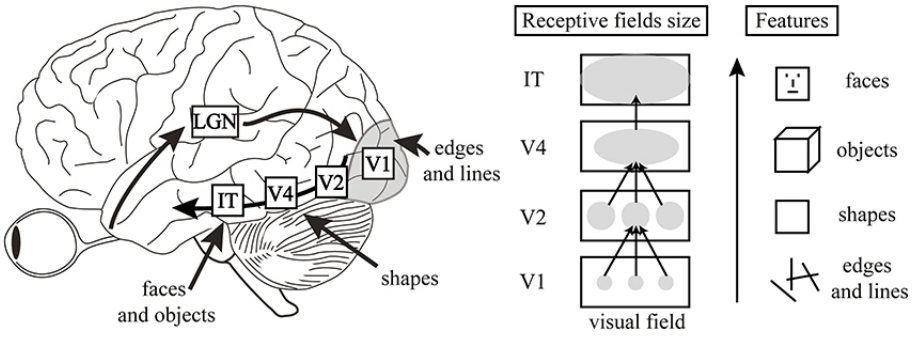

Figure 2: Hierarchical Processing in the Visual System [15].

Feature extraction with spatial invariance is also present in both the primate visual system and CNNs. At higher regions of the visual system hierarchy, receptive fields become larger, and retinotopic organization becomes less precise facilitating feature extraction with spatial invariance [14]. Since the filters of a CNN are applied across the entire input/feature map, CNN models are also capable of feature extraction with spatial invariance.

The baseline CNN architecture consisted of four convolutional layers, with 32, 64, 128, and 256 filters respectively, and configured to use padding that preserves the spatial dimensions of the input (i.e., padding='same'). The convolutional layers have kernels of size 7x7, 5x5, 3x3, and 3x3 respectively. Larger filter sizes are used in earlier layers to increase the receptive field of the network. Having a large receptive field is crucial for this classification task since the images the model is classifying are spectrograms from 4 EEG signals stacked on top of each other to form a single, 1-dimensional image. Since accurate classification of brain activity often requires features from all 4 EEGs of the image, having a large receptive field will help with more accurate classification. All model variations were run 5 times for 10 epochs, at a learning rate of $1e^{-3}$, using the Adam optimizer. The model architecture can be viewed in Table 2.

3.2 Model Interventions

Model interventions were made to the baseline CNN model to evaluate the impact of biologically-inspired components. The biological modifications include neuron adaptation, lateral connections, feed-forward skip connections, and only detecting lines and edges in the first stage.

3.2.1 Neuron adaptation

Neuron adaptation was introduced to the baseline CNN model by introducing L2 normalization by setting the weight_decay parameter to $1e^{-3}$ in the Adam optimizer. This mirrors the biological function of neuron adaptation, where neurons self-regulate to mitigate outlier effects. Incorporating an

Table 2: Baseline CNN Architecture

Layer (Type)	Output Shape	Kernel Size	Padding	Additional Info
Conv2d-1	[1, 32, W, H]	7x7	same	BatchNorm2d-1, ReLU, MaxPool2d with kernel size 2
Conv2d-2	[32, 64, W/2, H/2]	5x5	same	BatchNorm2d-2, ReLU, MaxPool2d with kernel size 2
Conv2d-3	[64, 128, W/4, H/4]	3x3	same	BatchNorm2d-3, ReLU, MaxPool2d with kernel size 2
Conv2d-4	[128, 256, W/8, H/8]	3x3	same	BatchNorm2d-4, ReLU, MaxPool2d with kernel size 2
AdaptiveAvgPool2d	[256, 1, 1]	-	-	-
Linear (fc1)	[256, 50]	-	-	ReLU
Linear (fc2)	[50, 6]	-	-	-

L2 normalization prevents any single neuron activation from becoming disproportionately influential, similar to how sensory neurons adjust their responsiveness based on the intensity of stimuli. This proposed method aims to improve the robustness of the CNN and to align the functionality more closely with the adaptive processes observed in biological neural systems.

3.2.2 Lateral connections

Self-attention layers were introduced to simulate lateral connections in the primate visual system, which facilitate contextual integration and enhance certain features by linking columns of neurons in the same cortical area, and allowing neurons to influence each other's responses. In the CNN, self-attention allows different regions of a feature map to interact, computing attention scores that weigh features based on their relationship to each other. This process helps the network emphasize more relevant features in the context of the entire input image/feature map, although it does not directly suppress nearby features like in the visual system [9].

The self-attention layers were inserted after the third and fourth convolutional layers in the CNN (memory constraints resulted in the removal of the self-attention layers after the first and second layers). The self-attention layers consist of key, query, and value matrices generated from the feature maps. The attention scores are calculated from the dot product of the query with all keys, multiplied by the value matrix, and added to the original input, resulting in contextually enhanced features.

3.2.3 Feed-forward Skip Connections

Feed-forward skip connections were implemented into the baseline CNN to better simulate the reutilization of features that occur in the primate visual system. In the visual cortex, early-detected, simple features are not discarded, but rather continuously integrated into the processing of subsequence, more complex stages. To replicate this biological process, the DenseNet architecture was implemented, which uses feed-forward skip connections to concatenate feature maps from all preceding layers to each subsequent layer, promoting the reuse of features, reducing the redundancy of relearning features since low-level features can directly contribute to the final output, and also making the model more parameter-efficient [13].

3.2.4 Vertical and Horizontal Line Filters

Two manually configured horizontal and vertical line filters were introduced within the first convolutional layer of the CNN to reflect visual processing observed in the primary visual cortex (V1) of primates. These modifications are designed to create 7x7 kernels that detect vertical, and horizontal lines. This is similar to the simple cells responding exclusively to edges and bars at certain orientations, as shown in Figure 3. The goal is to mirror this biological process and allow the model to differentiate between lines with greater accuracy.

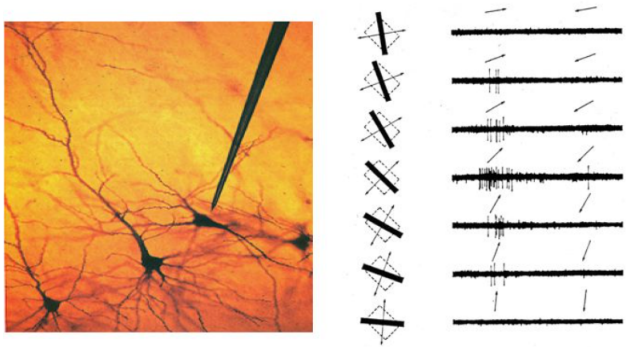

Figure 3: Direction Selectivity in V1 [16].

3.3 Kullback Leibler Divergence

The Kullback-Leiber (KL) divergence is a type of statistical divergence that measures how one probability distribution, P, is different from a second target probability distribution, Q. Outputs of the CNN model are probabilities obtained from softmax, and KL divergence measures how closely the predicted probabilities match the target probabilities. The lower the loss, the more closely the predicted probabilities resemble the expected target distributions.

$$D_{KL}(P \parallel Q) = \sum_{x \in \mathcal{X}} P(x) \log \left(\frac{P(x)}{Q(x)} \right)$$

4 Results

4.1 Baseline CNN

The baseline model achieved an average final training loss of 0.7034 and a validation loss of 0.8717, indicating a reasonably good fit without significant overfitting, as shown in Figure 4. To illustrate the predicted versus true probabilities, histograms were generated across different classes to reveal insights into the baseline model's classification performance, demonstrated in Figure 5.

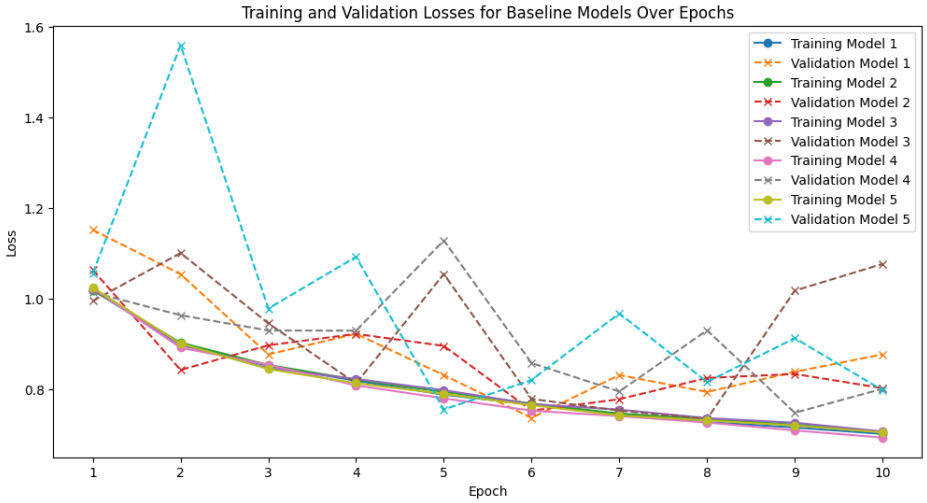

Figure 4: Baseline CNN Training and Validation Loss over Epochs.

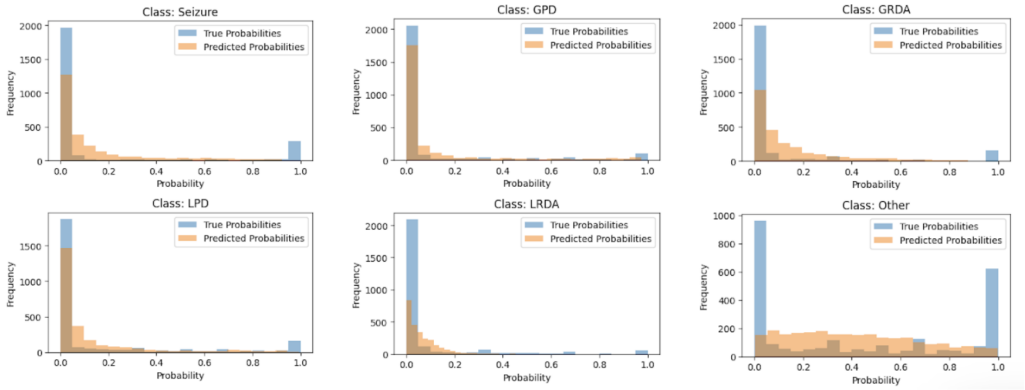

Figure 5: Baseline CNN Class Histograms.

4.1.1 Neuron adaptation

Adding L2 regularization resulted in a higher training loss than the baseline, but a lower validation set loss, and also overfit to the training data less than the baseline model, as shown in Figure 6. The average train and validation losses were 0.7842 and 0.8583 respectively. A slightly higher training set loss, and a slightly lower validation set loss is expected when adding regularization since the penalization of large weight results in the model being less likely to learn the noise in the training data, and fitting perfectly to the training data. As a result, the model's generalization capabilities improved, reflected in the lower validation loss.

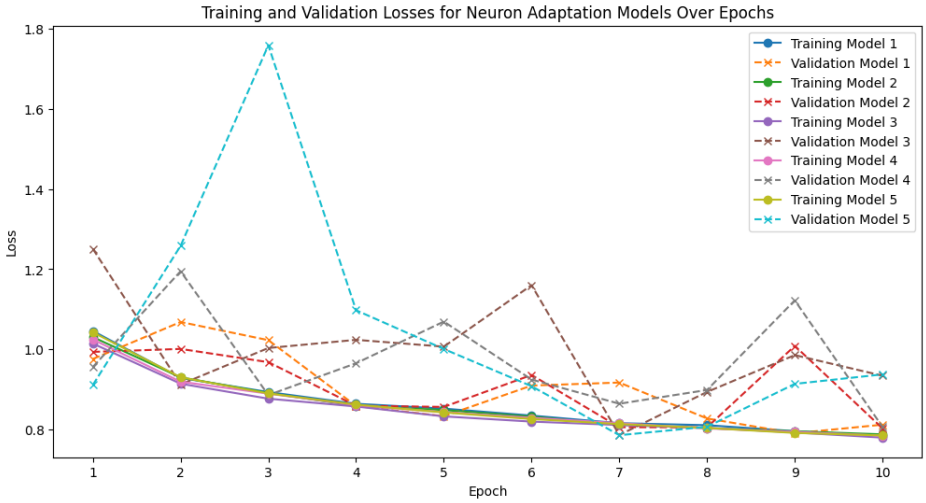

Figure 6: CNN + Neuron Adaptation Training and Validation Loss over Epochs.

4.1.2 Lateral connections

Adding lateral connections by including self-attention layers after the third and fourth convolutional layers yielded significant improvements to both the average train and validation losses with averages of 0.6535 and 0.7049 respectively. This model also demonstrated the best generalization capabilities out of all the adapted models by achieving the lowest loss on the validation set. The training and validation loss over 10 epochs for 5 model instances is shown in Figure 7.

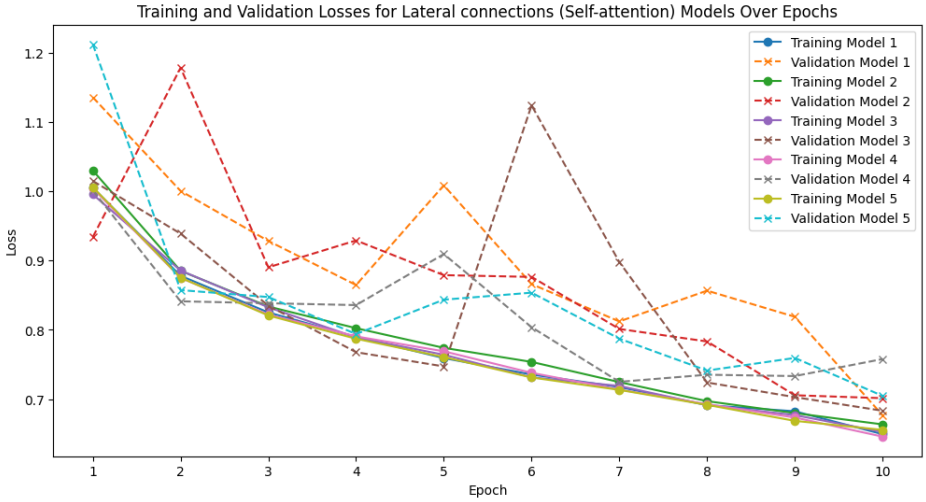

Figure 7: CNN + Lateral connections (self-attention) Training and Validation Loss over Epochs.

4.1.3 Feed-forward Skip Connections

Adding feed-forward skip connections yielded significant improvements to both the average train and validation losses with 0.6094 and 0.7538 respectively. However, with the validation loss being notably higher than the training loss, the model could benefit from regularization techniques such as L2 regularization applied for the neuron adaptation model. The training and validation loss over 10 epochs for 5 model instances is shown in Figure 8.

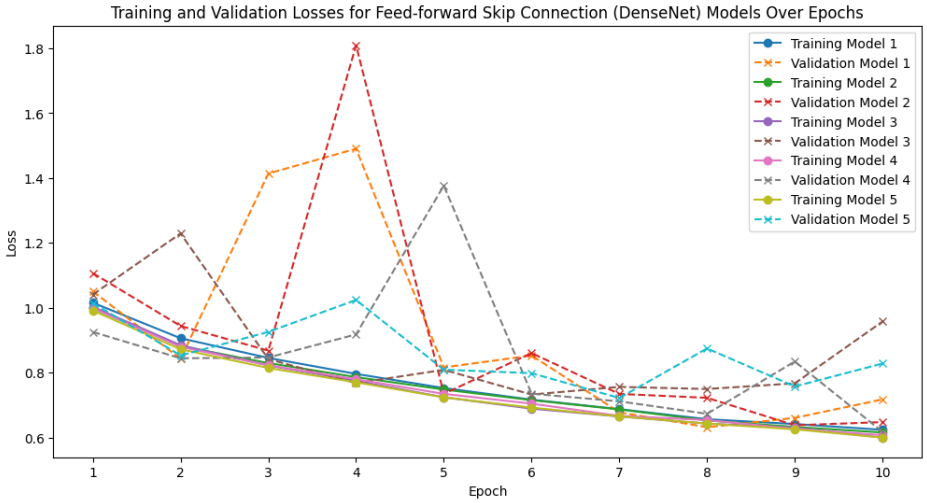

Figure 8: CNN + Feed-forward skip connections Training and Validation Loss over Epochs.

4.1.4 Vertical and Horizontal Line Filters

The manual filters created achieved training and validation losses of 0.6899 and 0.8087, respectively. An examination of the loss trends over epochs reveals a discernible decrease in the validation loss, with notable validation loss inconsistencies over all epochs. The training and validation loss over 10 epochs for 5 model instances is shown in Figure 9.

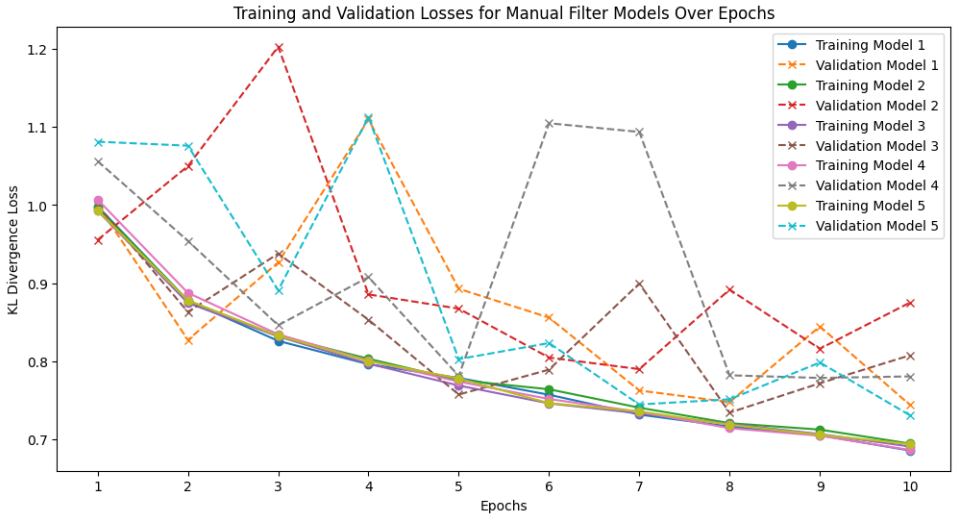

Figure 9: CNN + Manual Filters Training and Validation Loss over Epochs.

5 Discussion

The KL loss of the models: Baseline CNN, CNN + Neuron Adaptation, CNN + Lateral Connections, CNN + Feed-forward skip connections, and CNN + Manual Filters in predicting the harmful brain activity classes were evaluated. The results, as seen in Table 3, show that the validation loss for all models was relatively low compared to the baseline CNN. The CNN + Lateral connection model yielded the lowest validation loss, at a value of 0.7049, resulting in a 19.14% decrease in loss compared to the baseline CNN. The CNN + Neuron adaptation yielded the least significant difference in validation loss of 0.8583, resulting in only a 1.54% decrease in loss compared to the baseline CNN.

Table 3: Loss Comparison Between Models

Model	Train Loss	Validation Loss
CNN (baseline)	0.7034	0.8717
CNN + Neuron adaptation	0.7817	0.8583
CNN + Lateral connections	0.6535	0.7049
CNN + Feed-forward skip connections	0.6094	0.7538
CNN + Manual Filters	0.6899	0.8087

5.1 Neuron adaptation

Adding L2 regularization yielded the highest validation loss out of all the modifications made to the network, and also overfit to the training data the least out of all models. L2 regularization works by adding a penalty term to the loss function proportional to the sum of the squares of all the weights in the network, which penalizes larger weights. The resulting smaller weights of the model are less sensitive to minuscule changes in the input, which helps with generalization to the unseen data in the validation set. Smaller weights also limit the amount that the model will fit to the noise in the training data, reducing the amount of overfitting to the training data and improving the robustness of the model. The results yielded a higher training loss of 0.7817 compared to the baseline of 0.7034, likely as a result of discouraging the model from fitting the training data too closely. This yielded a slightly lower validation loss of 0.8583 compared to the baseline CNN of 0.8717.

The concept of neuron adaptation, inspired by neurobiological mechanisms, aligns with the principles of L2 regularization to stabilize the learning process. Translating this mechanism into machine learning models provides a dynamic form of regularization. Neuron adaptation in computational models is similar to the self-regulating capacity of biological systems, smoothing the learning trajectory and ensuring model robustness amidst diverse sensory inputs, as evidenced in prior studies [7]. By drawing parallels with these natural processes, L2 regularization not only enhances model performance but also provides a biologically informed mechanism for improved generalization and stability in learning tasks. However, the results demonstrate only a slight increase in model performance.

5.2 Lateral connections

The addition of self-attention layers after the third and fourth convolutional layers to simulate lateral connections in the primate visual system showed significant improvements compared to the baseline CNN, especially for the validation loss yielding a value of 0.7049. Receiving feature information from a broader context is crucial for the classification of EEG spectrograms, especially for the way that the data is formatted in this task, with 4 spectrograms representing reading from different brain regions stacked on top of each other to form one, 1-dimensional image. Accurate classification of these spectrograms often involves considering information from the entire input space, which the self-attention layers enable the CNN to do. Furthermore, the added ability to enhance important, key features and suppress irrelevant details that comes with the addition of the self-attention layers also results in a more generalized understanding of the data, thereby reducing overfitting and optimizing performance on the validation set.

5.3 Feed-forward Skip Connections

The incorporation of feed-forward skip connections into the baseline CNN model, mimicking DenseNet architecture, was observed to have a notably positive impact on model performance, yielding a validation loss of 0.7538. Despite having the same architecture as the baseline CNN, a small increase in parameters from adding the skip connections resulted in a large decrease in loss, demonstrating the model's increased parameter efficiency. Furthermore, while feed-forward skip connections contribute to a more robust internal representation of features, they alone do not prevent the model from overfitting, evident from the significant disparity of the validation loss from the

training loss. However, feed-forward skip connections evidently result in the model predicting more similarly to the expert annotator's targets, and as such should be kept as a biologically-inspired mechanism within CNN architectures for this EEG spectrogram classification task.

5.4 Vertical and Horizontal Line Filters

The manual filters created were designed to detect generic lines and edges. This improved generalization by decreasing validation loss, however, showed little improvement for the train loss. With trainable filters in the first layer, the model will learn features that are better adapted for the classification of EEG signals - these learned filters likely include, but are not limited to lines and edges of various orientations. Furthermore, with significantly fewer total filters in the first layer, the manually created filters were not able to capture the necessary variations present in the EEG spectrograms. Both of these factors contributed to the minimal decrease in training loss to a value of 0.6899.

Although lines and edges are detected in the first region (V1) of the primate visual system, there are considerably more orientations the neurons present in this region are receptive to compared to the number of filters in the CNN. With the number of filters used in the first layer of the CNN representing only a small fraction of the number of patterns detected in the V1 region, the CNN needs to compensate by tailoring its filters to be less generalized, but more relevant for the specific task at hand in order to achieve similar classification distributions.

Furthermore, reducing the number of filters in the first layer from 32 to 2, and having significantly fewer trainable parameters reduces the model complexity. A simpler model is less likely to learn the noise in the training data, leading to less overfitting and potentially better performance on the validation data, as demonstrated by the decrease in validation loss to 0.8087.

5.5 Final Model Recommendation

After all the biological aspects were separately evaluated, a final model can be built with all the beneficial additions - Neuron adaptation (L2 regularization), Lateral connections (self-attention), Feed-forward skip connections (DenseNet architecture), and CNN + Manual Filters. However, we recommend investigating further into the types of filters that can be added to the CNN network to better suit the classification task.

5.6 Future Work

Future work done for this classification task can first start with increasing the number of self-attention layers added after convolutional layers. The self-attention layers had the most significant impact on validation loss, but only two were added (after the third and fourth convolutional layers) due to limited memory capacity. With additional memory, adding the self-attention layer after every convolutional layer is likely to decrease the train and validation losses even further.

Since fewer trainable parameters when filters were set manually significantly decreased the validation loss, future work can also include adding these biological aspects to a baseline model with fewer trainable parameters. This can be accomplished by reducing the number of layers, the number of filters in each layer, or the filter sizes (although having a large receptive region was shown to be important for this task).

In addition, there are many more biological aspects that can be added to a CNN than the ones covered in this paper, and therefore are several directions future work on this classification task can proceed. One notable modification is to create a CNN that builds a salience map to facilitate feature selection and strengthen the detection of important features. Furthermore, a Recurrent-CNN can be implemented to simulate the top-down processing that occurs in the primate visual system.

Other changes can be made to the hyperparameters of the model, in order to find a set that yields the lowest loss. Tests can be conducted to find the optimal values for learning rate, CNN layers and filters,

and L2 regularization amount. Since the training and validation losses are still trending downwards in all models by epoch 10, the number of epochs can be increased as well to further decrease training and validation loss.

6 References

[1] G. A. Light et al., "Electroencephalography (EEG) and event-related potentials (erps) with human participants," Current protocols in neuroscience, https://www.ncbi.nlm.nih.gov/pmc/articles/PMC2909037/ (accessed Apr. 22, 2024).

[2] E. K. St. Louis, "Electroencephalography (EEG) Introduction," Electroencephalography (EEG): An Introductory Text and Atlas of Normal and Abnormal Findings in Adults, Children, and Infants [Internet]., https://www.ncbi.nlm.nih.gov/books/NBK390346/ (accessed Apr. 22, 2024).

[3] "HMS - Harmful Brain Activity Classification," Kaggle, https://www.kaggle.com/competitions/hms-harmful-brain-activity-classification/overview (accessed Apr. 23, 2024).

[4] S. Kullback and R. A. Leibler, "On information and sufficiency," Project Euclid, https://projecteuclid.org/journals/annals-of-mathematical-statistics/volume-22/issue-1/On-Information-and-Sufficiency/10.1214/aoms/1177729694.full (accessed Apr. 22, 2024).

[5] Metric, "Kullback Leibler divergence," Kaggle, https://www.kaggle.com/code/metric/kullback-leibler-divergence/notebook (accessed Apr. 23, 2024).

[6] F. Bertoni, G. Citti, and A. Sarti, "LGN-CNN: A biologically inspired CNN architecture," Neural Networks, vol. 145, pp. 42–55, Jan. 2022. doi:10.1016/j.neunet.2021.09.024

[7] Y. Kubo, E. Chalmers, and A. Luczak, "Biologically-inspired neuronal adaptation improves learning in Neural Networks," Communicative; Integrative Biology, vol. 16, no. 1, Jan. 2023. doi:10.1080/19420889.2022.2163131

[8] N. Kanwisher and E. Wojciulik, "Visual attention: Insights from brain imaging," Nature News, https://www.nature.com/articles/35039043 (accessed Apr. 22, 2024).

[9] E. R. Kandel, J. H. Schwartz, et al., Eds., Principles of Neural Science, Fifth Edition. 5th ed.

[10] G. W. Lindsay, "Attention in psychology, neuroscience, and Machine Learning," Frontiers in Computational Neuroscience, vol. 14, Apr. 2020. doi:10.3389/fncom.2020.00029

[11] Are skip connections necessary for biologically plausible ..., https://openreview.net/pdf?id=SJgHEQYLUS (accessed Apr. 23, 2024).

[12] J. D. Semedo et al., "Feedforward and feedback interactions between visual cortical areas use different population activity patterns," Nature News, https://www.nature.com/articles/s41467-022-28552-w (accessed Apr. 22, 2024).

[13] W. Huang, G. Peng, and X. Tang, A limit of densely connected convolutional networks V1, Oct. 2019. doi:10.17504/protocols.io.8j6hure

[14] V. K. Berezovskii, J. J. Nassi, and R. T. Born, "Segregation of feedforward and feedback projections in mouse visual cortex," The Journal of comparative neurology.

[15] M. H. Herzog and A. M. Clarke, "Why vision is not both hierarchical and Feedforward," Frontiers, https://www.frontiersin.org/articles/10.3389/fncom.2014.00135/full (accessed Apr. 22, 2024).

[16] "Perception lecture notes: Secondary cortical visual areas and the what/where pathways," Perception Lecture Notes: Cortical Visual Areas and Pathways, https://www.cns.nyu.edu/ david/courses/perception/lecturenotes/what-where/what-where.html (accessed Apr. 22, 2024).